OFFICE OF NAVAL RESEARCH

Grant N00014-89-J-1178

R&T Code 413Q001-05

TECHNICAL REPORT No. #47

Spectroscopic Differential Reflectance as an Analytical Probe for Microelectronic Processing

By:

T. M. Burns and E. A. Irene
Department of Chemistry
University of North Carolina at Chapel Hill
Chapel Hill, NC 27599-3290

S. Chevacharoeukul, G. E. McGuire
MCNC, Research Triangle Park, NC 27709

Submitted to:

Journal of Vacuum Science and Technology B

July 13, 1992

REPORT DOCUMENTATION PAGE

Form Approved
OMB No. 0704-0188

1. AGENCY USE ONLY (Leave blank)	2. REPORT DATE	3. REPORT TYPE AND DATES COVERED
	July 13, 1992	

4. TITLE AND SUBTITLE
Spectroscopic Differential Reflectance as an Analytical Probe for Microelectronic Processing

5. FUNDING NUMBERS
#N00014-89-J-1178

6. AUTHOR(S)
T. M. Burns, E.A. Irene, UNC-CH
S. Chevacharoeukul, G.E. McGuire - MCNC, RTP, NC

7. PERFORMING ORGANIZATION NAME(S) AND ADDRESS(ES)
The University of North Carolina
Chemistry Department
CB# 3290, Venable Hall
Chapel Hill, NC 27599-3290

8. PERFORMING ORGANIZATION REPORT NUMBER

9. SPONSORING/MONITORING AGENCY NAME(S) AND ADDRESS(ES)
Office of Naval Research
800 N. Quincy Street
Arlington, VA 22217-5000

10. SPONSORING/MONITORING AGENCY REPORT NUMBER
Technical Report #47

11. SUPPLEMENTARY NOTES
none

12a. DISTRIBUTION/AVAILABILITY STATEMENT
This document has been approved for public release and sale, distribution of this document is unlimited.

12b. DISTRIBUTION CODE

13. ABSTRACT *(Maximum 200 words)*

It is important in microelectronics to be able to measure damage and monitor processing during or following the many different processes. To this end, a simple and universal technique is desirable. In this paper differential reflectance, DR, is examined as a tool for studying several processes including implantation, preamorphization, solid phase epitaxy, and rapid thermal annealing. DR is found to be able to measure small differences between samples, and the amount of damage is qualitatively assessed by the intensity and broadening of the silicon interband transitions. More quantitative information about damage layer thickness can be obtained if interference bands are present. DR results were in good agreement with transmission electron microscope, TEM, findings, and in some cases DR spectra suggested residual damage where TEM found annealing to be complete. Preamorphized samples had different interband transition peak broadening and responded differently to annealing compared to their non-preamorphized counterparts. Distinctive DR spectral features were also obtained for heavily doped silicon samples, and the features were related to dopant species size.

14. SUBJECT TERMS	15. NUMBER OF PAGES
differential reflectance, damage in thin films	16. PRICE CODE

17. SECURITY CLASSIFICATION OF REPORT	18. SECURITY CLASSIFICATION OF THIS PAGE	19. SECURITY CLASSIFICATION OF ABSTRACT	20. LIMITATION OF ABSTRACT
unclassified	unclassified	unclassified	

Spectroscopic Differential Reflectance as an Analytical Probe for Microelectronic Processing

T.M.Burns, E.A.Irene
University of North Carolina - Chapel Hill
Chapel Hill, NC 27599-3290

S.Chevacharoeukul, G.E.McGuire
MCNC, Research Triangle Park, NC 27709

ABSTRACT

It is important in microelectronics to be able to measure damage and monitor processing during or following the many different processes. To this end, a simple and universal technique is desirable. In this paper differential reflectance, DR, is examined as a tool for studying several processes including implantation, preamorphization, solid phase epitaxy, and rapid thermal annealing. DR is found to be able to measure small differences between samples, and the amount of damage is qualitatively assessed by the intensity and broadening of the silicon interband transitions. More quantitative information about damage layer thickness can be obtained if interference bands are present. DR results were in good agreement with transmission electron microscope, TEM, findings, and in some cases DR spectra suggested residual damage where TEM found annealing to be complete. Preamorphized samples had different interband transition peak broadening and responded differently to annealing compared to their non-preamorphized counterparts. Distinctive DR spectral features were also obtained for heavily doped silicon samples, and the features were related to dopant species size.

Introduction

Microelectronics processing involves a number of process steps that can create damage or otherwise alter the sample. Oftentimes a simple comparative technique is needed to determine any deviation from the desired standard in a fabrication process. Differential reflectometry, DR, directly measures the optical reflectance difference between a sample and a reference (1). By measuring the difference, small changes in the near surface optical properties resulting from damage, film growth, etching, and impurities become detectable. DR has been used successfully to study alloy ordering and corrosion (2), $TiSi_2$ growth on silicon (3), the etching of silicon oxides (4), and the damage of silicon surfaces induced by ion implantation including the study of buried layers (5-7). The technique is conceptually simple compared to other techniques such as ellipsometry that also sensitively measures optical properties of a surface.

In this paper we present DR results on Si surface damage caused by low energy implantations commonly used in processing submicron-scale devices. In addition we report that DR is sensitive to changes caused by preamorphization, annealing, high concentrations of dopants, and damage below detection limits of transmission electron microscopy (TEM). When this new information is added to the previous work using DR, studies of some of these samples by TEM, secondary ion mass spectrometry (SIMS), and electrical measurements (8,9), the technique emerges as a nearly universal, sensitive process monitoring tool. It also has the benefits of being a fast and non-destructive sampling method.

II. Experimental

A. Sample Preparation

For the DR studies reported here, many different sample preparations were used, and are identified in Tables I and II. The left most column in Tables I and II contains the sample number referred to in the spectra that follow. The remaining columns indicate whether and under what conditions a process step such as implantation, solid phase epitaxy, SPE, or rapid thermal anneal, RTA, took place.

Table I describes samples that represent several factors associated with ion implantation. Sample #1 had oxygen, O_2^+, implanted through two surface films prior to film removal. Sample #2 is used to verify that an oxide film on the surface does not contribute to the observed damage. Samples #3 and #4 each have the same implant, but sample #4 has a portion of the damaged region etched away to expose the highest concentration of the implantation profile at the surface. Samples #5-9 were preamorphized with germanium, and then samples #6-9 were implanted with different doses of 25 keV germanium.

Table II contains samples that were preamorphized as well as some that were not for comparison, and some that were annealed. There were two types of annealing used: all of the annealed samples underwent solid phase epitaxy, SPE, for 30 minutes first at 450^o and then again at 550^{o}C, and some of these underwent rapid thermal anneal, RTA, for 10 seconds at a temperature specified in the table. The samples in Table II can be divided into three groups: BF_2^+ implanted samples annealed at different temperatures with half the samples having Ge^+ preamorphization (samples #10-21), As^+ implantation annealed at different temperatures (samples #22-25), and Si^+ preamorphization followed by implants of BF_2^+ or As^+ (samples #26, #27). The As^+ implanted samples are influenced by the large size of the arsenic compared to silicon so that As in large concentrations disrupts the

silicon lattice. Table III contains several studied samples which were not implanted, but had different background doping. These samples distinguished by resistivity that is inversely related to the dopant concentration, were included to examine the effect of dopant size and concentration.

B. Measurements

The DR apparatus used is shown in Figure 1 and described in detail elsewhere (1,4) requires placing two samples side by side and rastering the incident light across each sample at near normal incidence. Also, the incident wavelength is scanned from 200-800 nm, and the reflected light is detected using a photomultiplier tube and lock-in amplifier to extract the difference in reflectance between the two samples. This difference is then divided by the average reflectance as obtained from a low pass filter to obtain a normalized difference in reflectance:

$$\frac{\Delta R}{R} = \frac{R_1 - R_2}{\bar{R}} \qquad (1)$$

where R_1 and R_2 are the reflectance from each sample, respectively. The spectra are plotted as dR/R vs. the wavelength of the impinging light.

If the two adjacent samples in the DR apparatus are identical, then the measured difference would be zero for all the wavelengths. The reflectance of crystalline silicon, c-Si, contains several interband transitions including two peaks at 272 nm (4.2 eV) and 368 nm (3.4 eV). When a sample is damaged it is well described by a combination of the optical values of c-Si and amorphous silicon, a-Si, which unlike c-Si is a smooth function of

wavelength. Compared to a c-Si reference the damaged silicon will yield a DR spectra containing the c-Si interband features. The more damaged a sample is the more its optical properties will resemble a-Si and the larger the difference spectra will be compared to an undamaged, or c-Si, reference. A second feature that may be present in DR spectra is interference bands resulting from films on the surface of one or both samples. These bands appear at wavelengths longer than 400 nm, and the exact position is dependent on the film thickness. Simulations of the DR spectra can be performed using the optical properties of the substrates and films (10). The measured spectra have a sensitivity limit close to 1% difference in reflectance determined primarily by noise and instrumental artifacts. Thus, samples with thin damage layers differing by 0.1 nm can be distinguished. Samples with less than 1% difference would be optically indistinguishable, and judged to be the same. An additional point to make is that the spectra can be plotted with the peaks upward or downward, depending on which side of the stage each sample is on and the lock-in amplifier's phase; a different representation is used, for example, in Figure 9 of this paper.

III. Results and Discussion

A. Implantation Damage

These samples along with those in previous papers (5-7) show how DR can be used to study and evaluate implantation damage. Here the reference can be selected to eliminate, through comparison, possible effects from other processing steps. Figure 2 contains two DR spectra. Spectrum (a) compares the implanted sample #1 to a reference similarly processed except for the implantation. Seen in the spectrum are large interband transition peaks at 270 and 360 nm resulting from damage caused by the tail of the O_2^+

implant profile into the substrate of #1. This region, which is now the surface, contains small point defects which are below the detectable level for TEM. Spectrum (b) compares the reference of (a) with an out of the box silicon wafer, and it can be seen that this spectrum is without spectral features. Similar to this comparison is that shown in Figure 3 in which sample #2 had a 10 nm oxide grown at 950°C and then removed by an HF dip. For a reference, an out of the box silicon wafer was dipped in HF to eliminate any effects from this treatment in the comparison. This spectrum like that of spectrum (b) in Figure 2 is featureless and shows that DR could not detect any difference in reflectance and therefore no substantial damage caused by an oxide film. Oxide growth on surfaces is known to generate a silicon interstial rich area at the surface of the substrate, but this effect was not measurable. Some optical effects from surface oxide formation may actually exist but are too small to be definitively measured by DR with the 1 % sensitivity of our instrument, while the effects of point defects below the surface are easily measured.

Two wafers, #3 and #4, were implanted with 85 keV Ge at a dose of $10^{15}/cm^2$ forming a surface amorphous layer. The interface was found by TEM to be 97 nm deep (9). Sample #4 was then wet etched leaving an amorphous layer of 57 nm. Figure 4a shows a large difference between the surfaces of these two samples where sample #3 exhibits greater damage than #4 as determined by the direction (up or down) of the interband transition peaks, the sample position, and the lock-in amplifier's phase. In order to understand the meaning of this difference it is necessary to know the depth reached by the probing light. For $I/I_O = e^{-1}$ this mean penetration depth, MD, can be expressed by

$$MD = \frac{\lambda}{4\pi k} \qquad (2)$$

where λ is wavelength and k is the absorption constant for a given material at a given wavelength. Using this equation and the optical constants for a-Si and c-Si (11) we can calculate the mean penetration depth for the light into these samples. It is found that the depth into a-Si for λ in the range of 200 and 400 nm is between 6 and 15 nm, and gradually increases to 600 nm at λ = 800 nm. This means that the interband transition region, $\lambda <$ 400 nm, the light does not probe the interface region of either sample, #3 or #4, but that these peaks must arise from a difference in the level of amorphization. This is interesting, since there is some controversy on whether or not there are levels of damage above the threshold for amorphization. At longer wavelengths where DR probes to the interface, interference band is found at 600 nm.

For comparison with the spectrum in Figure 4a, simulated differences between a 60 nm a-Si layer on c-Si and a c-Si reference is shown in Figure 4b. The spectral features at the interband transitions at 280 and 368 nm are nearly identical as is the broad band near 600 nm due to interference film thickness. The latter results from constructive interference of the impinging light from the different interfaces of the film and substrate and the position depends on the thickness of film (distance between the interfaces). The band at 600 nm corresponds to a thickness of about 60 nm, and this is confirmed by TEM which measured a thickness of 57 nm for sample #4. Amplitude differences between Figures 4a and 4b can have several causes ranging from an experimental intensity loss to varying optical constants for the films which must be estimated as some combination of a-Si and c-Si. The more c-Si

like the film is, the more attenuated the spectral peaks will be, so if compared to a model using a-Si optical values this film would result in lower amplitude features. To complicate matters, each of the samples being compared in this case have different and unknown optical constants depending on the amount of damage. Therefore a quantitative interpretation for the DR spectra is not possible at this time except for the estimate of film thickness from the band near 600 nm.

B. Annealing

Annealing an ion damaged sample decreases the DR amplitude relative to an undamaged sample. This is easy to understand, since DR measures the average damage in the probed region and annealing generally decreases the number of defects. For the process of solid phase epitaxy (SPE), which regrows amorphized silicon, DR would be predicted to yield changes in the interference band region (400-800 nm) of the spectrum that are indicative of a shifting interface effect as the top amorphous layer converts back to crystalline with the expected decrease in total damage represented by a reduction in DR amplitude. Rapid thermal annealing (RTA) employs higher temperatures and shorter periods of heating to repair lattice damage, with as little diffusion as possible, which results in a decreasing dR/R amplitude, particularly in the silicon interband transition region (200-400 nm). All of the implanted samples studied underwent SPE at 450°C for 30 minutes and then at 550°C for 30 minutes, and some samples then underwent RTA (8). Thus, we do not examine the effects of SPE alone with DR, but instead we observe the role of temperature in RTA with maximum temperatures at 1050°C and each exposure lasting 10 seconds.

As shown in Table II, samples #10 - 15 were preamorphized with Ge^+, implanted with BF_2^+, and annealed. The initial amorphous surface region has a thickness of around 36 nm as measured from TEM micrographs, while samples #16 - 21 were implanted without preamorphization yielding an amorphous depth of about 23 nm as determined by TEM. Samples #10 and #16, from each group, did not undergo RTA and the DR spectra are shown compared to a RCA cleaned silicon reference sample in Figure 5. Spectra (a) and (b) display a different peak shape at 366 nm that can be attributed to the difference in the damage depth or the level of defects created. #10 which underwent premorphization is damaged deeper and also may have more damage sites due to contribution from Ge. The contribution from the size of Ge relative to the lattice has been ruled out, because ions of similar size and concentration show no effects. The other samples were examined by comparing the unannealed sample, #10 or #16, to the corresponding samples, #11-15 and #17-21, respectively, that underwent different RTA treatments. Figure 6 summarizes these comparisons. Non-preamorphized samples changed more by annealing at lower temperatures (<850°C) than preamorphized samples, as represented by a larger difference in comparison with its respective unannealed reference sample, #10 or #16. This is especially notable for the 750°C RTA sample. The preamorphized samples did not show significant improvement until 850°C in agreement with TEM studies of the preamorphized samples reported elsewhere (9). The reversal of peak heights between the two series seen at 1050°C is not significant, since the two series have different reference samples. The preamorphized series being more highly damaged have more damage to anneal out, thereby yielding a greater difference for the high temperatures anneals. Furthermore, there is little

change between the preamorphized samples annealed at 950 and 1050°C, suggesting that most of the damage was annealed out for this series by 950°C, while at 1050°C the non-preamorphized samples continued to improve. Recent TEM data for the preamorphized samples (9) showed that damage removal was almost complete at 950°C and complete at 1050°C. Direct comparison of the preamorphized samples to the non-preamorphized ones with the same heat treatment are shown in Figure 7. These spectra represent the difference in damage between the two processes as a function of the annealing temperature, and as stated above it is seen that the preamorphized samples (#10 - #14) contain greater damage at all annealing temperatures. As expected, the difference amplitude for the comparison of the samples with the lower temperature heat treatments was the greatest, since preamorphization has contributed measurable defects to one of the samples which have not been removed by annealing. As the temperature was increased the spectra for the two sets of samples became more alike. The DR comparison of samples #14 vs #20 was the pair with the smallest distinguishable difference; the comparison of samples #15 and #21 which were both annealed at 1050°C showed no distinguishable differences.

Another series of samples was As^+ implanted and annealed at different temperatures. In Table II, samples #22 - 25 were SPE regrown at 550°C for 30 minutes before undergoing RTA at temperatures of 850°, 950°, or 1050°C. Implantation left the samples with an interface depth of about 30 nm as found by TEM. #23 in Figure 8 which has the lowest RTA temperature of 850°C is very similar in amplitude to #22 which did not receive RTA treatment, but the spectra differs above 400 nm. Sample #1 previously showed DR's sensitivity to point defects below the interface, suggesting that here the annealing of

the point defects into fewer larger defects causes a difference in the light scattering from these centers which gives rise to a different interference features for #22 and #23. From Figure 8 it is seen that the comparisons of higher RTA temperatures exhibit decreased total damage as seen by the lower amplitudes of samples #24 and #25. These samples also exhibit the broad interband transition peaks at 286 nm and 368 nm corresponding to the 4.2 eV and the 3.4 eV band with the 368 nm being nearly twice as large as the 286 nm band. These features are also present in the other heavily doped samples, and suggests that large amounts of defects caused by implantation with large ions or double implants (preamorphized samples) leaves residual defects, even after annealing, which cause changes in the optical properties. It is interesting to note that TEM of this implant annealed at 950°C showed most of the damage to be annealed out (9), yet DR sees a clear optical difference.

C. Preamorphization

Samples #5 through #9 were preamorphized with 85 keV Ge at 10^{15} ions/cm^2. For samples #6 through #9 the preamorphization was followed by implantation with 25 keV Ge with doses ranging from $5x10^{14}$ to 10^{16} ions/cm^2. All the samples (#5-9) then underwent SPE and RTA heat treatments. The DR spectra of the samples in Figure 9 show residual damage from the preamorphization and implantation. Note that the spectra appear inverted relative to previous figures. This occurs when R_1 and R_2 in Equation 1 are reversed so that dR/R has the opposite sign. We use this representation here to illustrate that the divergence from dR/R = 0 is the important parameter. It is seen that the damage is greater for the samples that were implanted at higher doses. Two possible explanations for this are that

the higher dose implants require higher temperatures to anneal out the damage and/or that the large concentration of excess germanium ions in the lattice are measurable by DR. It is not likely that the concentration of Ge is that cause, since other samples presented here show this not to be a factor. The increase in damage, represented by the peak heights of the SDR spectra at 292 and 366 nm is plotted in Figure 10 as a function of log(dose) of the implant. This plot shows there is a linear relationship between the SDR peak height and the log(dose) of the implant. Dose is directly related to the concentration of the implanted species and the amount of damage remaining after anneal at 950°C. We will show later that large dopants in these concentrations do not contribute to the measurable differences.

Samples #10-16, whose peak heights are seen in Figure 6, show variations in the damaged silicon spectra consistent with the other preamorphized samples. The interesting feature in the spectra (not shown) is the interband transition peak at 370 nm (3.4 eV) which is asymmetrically broadened resulting in an effective peak shift to longer wavelength for non-preamorphized samples compared to the equivalent preamorphized samples. The 270 nm (4.2 eV) peak is very broad and lower in intensity compared to the 370 nm peak. There are no obvious interference bands for these samples. Once again
this demonstrates effects of increased point defects on the optical properties for preamorphized samples.

Each of samples #26 and #27 was preamorphized with Si before implantation with the respective ion. Both samples had an interface depth of approximately 34 nm determined by TEM. From the DR spectrum of each of these samples versus an unimplanted reference shown in Figure 11, it can be seen that #27 has an interband transition peak amplitude

about twice that of #26, suggesting greater damage in the sample. An examination of these two samples within Table II reveals that they were not implanted with the same energy or dose; instead, these parameters were adjusted to give similar concentration profiles following implantation and anneal. SIMS profiles of these samples (8) show the depth to be approximately the same, but the arsenic implant is almost an order of magnitude larger in concentration at the peak, possibly explaining the difference in SDR peak height. The larger size of the arsenic ion relative to boron and silicon may play a role, since arsenic causes more nuclear collisions that boron therefore creating more defects to which DR has been shown to be sensitive. Both spectra exhibit the features seen in the previous samples, specifically the large sharp peak at 366 nm while that at 273 is a broad peak of lower intensity. Also the arsenic implanted sample has its peak shifted slightly to 368 nm due to asymmetric broadening.

Samples #26 and #27 were also compared to samples #20 and #24, respectively, which are equivalent except for silicon preamorphization step. As with comparisons above, the peak height of #24 versus #27 was about 2 times that of #20 versus #26, but the peak is shifted to 380 nm for the former which is shown in Figure 12. An examination of #24 versus an untreated reference yields a peak position at 368 nm identical to #27 vs. the same reference, but a closer examination shows that the peak for #27 has a broader shoulder on the long wavelength side. When the two are compared this shoulder results in a peak at 380 nm (the difference between two similar peaks) determined by the extent of the asymmetric broadening of sample #27. DR peaks do not directly correspond to the interband transitions but rather to the difference between the interband transitions of two samples.

Therefore, a DR peak can result from a broadening of the interband transition peak of one sample with the DR peak position determined by the extent of broadening.

The effect of the size of the preamorphizing ion can also be examined by comparing the silicon pramorphized sample #26 and the germanium preamorphized sample #14 to sample #20 that did not receive preamophization. These comparisons show that #26 versus #20 and #14 vs #20 have virtually identical spectra, leading to the conclusion that the larger germanium ion does not affect the DR measurement of the optical properties.

D. Ion Concentration

The difference in concentration of minority constituents in a sample can be studied without the contribution from damage effects due to implantation by comparing samples with different background doping. When comparing samples with different dopant species but with similar resistivities, the spectrum is flat indicating no difference within the sensitivity of the instrument. Figure 13 contains four spectra of samples with different dopants and low resistivity, and therefore high dopant concentration (10^{18}), compared to a phosphorus doped n<100>Si of 2 ohm-cm resistivity (10^{15} ions/cm^2). It can be seen that these spectra are not flat but rather have various amplitude peak heights. It appears that the observed optical difference or damage results from the large concentration of ions in the lattice and the magnitude of the difference is related to the size of the ions relative to the host species. This intuitive notion is substantiated in Figure 14, where the peak heights from Figure 13 are plotted against the ionic radius multiplied by conductivity for each dopant. It was necessary to multiply the ion radius by the conductivity in order to normalize the samples for variations in dopant concentration. This linear relationship indicates the importance of

both size and concentration of the dopant. Comparisons with samples of higher resistivities in the range of 0.4 to 50 ohm-cm (10^{14} to 10^{16} ions/cm^2 concentration) gave no differences. This technique is shown to be sensitive to dopant size only at very large concentrations on the order of 10^{18} ion/cm^2.

IV. Summary and Conclusions

It has been shown that DR has sensitivity to many key parameters in various microelectronic processes. It is particularly well suited for comparing a processed sample to a standard, because the differential nature of the technique renders even small differences measurable, and at the same time the technique is fast and non-destructive. In this paper it has been shown that the position and relative intensity of the interband transitions can give information about the level of damage, as it was shown that both high ion concentrations and preamorphization result in featural shifts of interband transitions. The effectiveness of temperature in the removal of crystalline and amorphous damage was also discernable from DR spectra, and of particular note is the sensitivity to defects below the detection limit of TEM. In addition, information found by DR studies is in good agreement with TEM data and previous work with ellipsometry data (7). The limitation of this technique is that the information gained is largely qualitative because the relative comparison does not give any absolute values for standardization. Some more quantitative information can be gained, however, about the approximate thickness of overlayers, if interference bands are present.

Acknowledgements

The authors gratefully acknowledge the Office of Naval Research, ONR, the NSF Engineering Research Center at North Carolina State University, and MCNC for financial support.

References

1. J.A.Holbrook and R.E. Hummel; Rev Sci Instrum **44**(4), 463 (1973).

2. R.E.Hummel; Phys Stat Sol (a) **76**, 11 (1983).

3. M.Tanaka, P.E.Schmid, A.Piaggi, and F.Levy; J Vac Sci Technol **A** 7(6), 3287 (1989).

4. Uean-Sin Pahk, S.Chongsawangvirod, E.A.Irene; J Electrochem Soc, **138**(1), 308 (1991).

5. D.R. Hagmann, W.Xi, and R.E.Hummel; Ion Beam Modification of Materials Conference, Knoxville, TN, 1990.

6. R.E.Hummel, W.Xi, and D.R.Hagmann; Electrochem Soc Meeting, Oct 1989, Hollywood, Fl, Abs#422.

7. T.M.Burns, S.Chongsawangvirod, J.W.Andrews, E.A.Irene, S.Chevacharoeukel, G.McGuire; J Vac Sci Technol **B 9**, 41 (1991).

8. C.M.Osburn, S.Chevacharoeukul, G.E.McGuire; Proceedings of the 3rd Int. Sym. of ULSI, J.M.Andrews and G.K.Celler,eds. Electrochem. Soc., 1991, 330.

9. S.Chevacharoeukul, C.M.Osburn, G.E.McGuire; Proceedings of the 3rd Int. Sym. of ULSI, J.M.Andrews and G.K.Celler,eds. Electrochem. Soc., 1991, 285.

10. O.S. Heavens **Optical Properties of Thin Solid Films** (Dover Publ., Inc., New York, 1965) Chap. 4.

11. E.D.Palik, ed., **Handbook of Optical Constants of Solids** (Academic, Orlando, FL, 1985).

List of Tables:

Table I Implantation Samples

Sample #	Preamorphization	Implantation	Other Information
1	none	35 keV O_2 10^{15} ions/cm^2	Implanted through an oxide and poly films which are removed after implantation
2	none	none	10 nm oxide grown at 950°C and removed with HF dip
3	none	85 keV Ge 10^{15} ions/cm^2	Amorphous depth is 97 nm
4	none	"	Same as above, but etched to 57 nm of original depth
5	85 keV Ge 10^{15} ions/cm^2	none	SPE, RTA
6	"	25 keV Ge $5x10^{14}$/cm^2	"
7	"	25 keV Ge $1x10^{15}$/cm^2	"
8	"	25 keV Ge $5x10^{15}$/cm^2	"
9	"	25 keV Ge $1x10^{16}$/cm^2	"

Table II Preamorphized and Annealed Samples

Sample #	Preamorphization	Implantation	RTA*
10	25 keV Ge	8 keV BF_2	none
11	"	"	650°C
12	"	"	750°C
13	"	"	850°C
14	"	"	950°C
15	"	"	1050°C
16	none	8 keV BF_2	none
17	"	"	650°C
18	"	"	750°C
19	"	"	850°C
20	"	"	950°C
21	"	"	1050°C
22	none	15 keV As	none
23	"	"	850°C
24	"	"	950°C
25	"	"	1050°C
26	20 keV Si	8 keV BF_2	950°C
27	20 keV Si	15 keV As	950°C

* All samples were preannealed at 450°C/30 min followed by SPE at 550°C/30 min regardless whether or not they underwent RTA. All RTA treatments were for 10 seconds.

Table III Background Doped Samples

Dopant	Resistivity (ρ) ohm-cm	Ionic Radius (r) nm	r/ρ	DR Peak Height @366 nm
As^+	<0.006	0.222	37.0	1.064
Sb^+	0.005-0.02	0.245	20.4	0.690
P^+	0.018	0.212	11.8	0.520
B^+	0.010	0.023	2.3	0.240

List of Figures:

Figure 13. DR spectra of samples with background doping of different species and concentrations as related to resistivity and compared to n-P<100> silicon with resistivity, R, of 0.5 to 2.5/cm^2, a) n-As<100>, R < 0.006; b) n-Sb, R = 0.005-0.02; c) n-P, R = 0.018; d)p-B, R = 0.010.

Figure 14. Graph of DR peak heights from spectra in figure 13 versus ionic radii of the doping species normalized for differences in concentration.

DR Experimental Setup

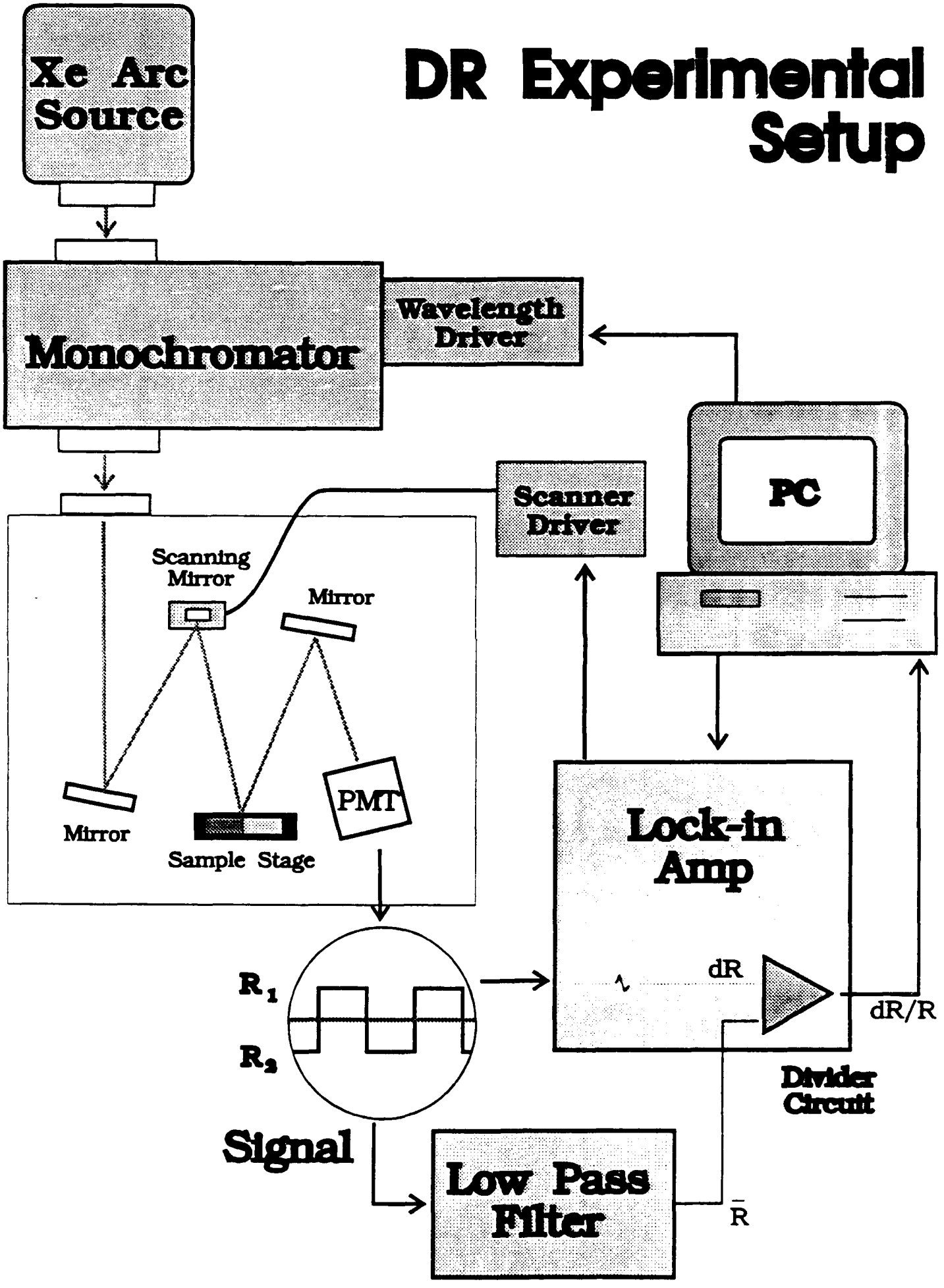

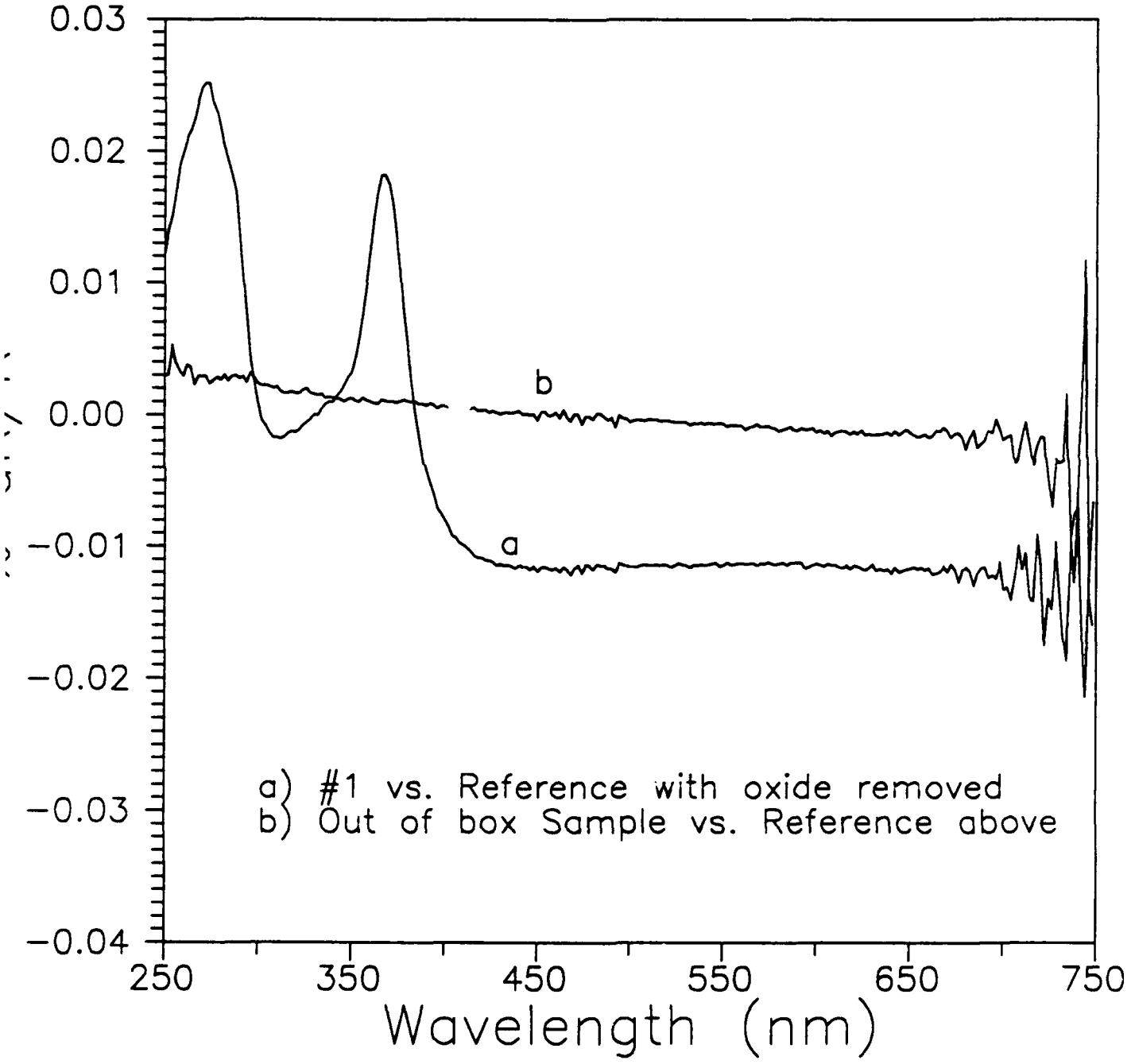
0.03
0.02
0.01
0.00
−0.01
−0.02
−0.03
−0.04
250
350
450
550
650
750
Wavelength (nm)
b
a
a) #1 vs. Reference with oxide removed
b) Out of box Sample vs. Reference above

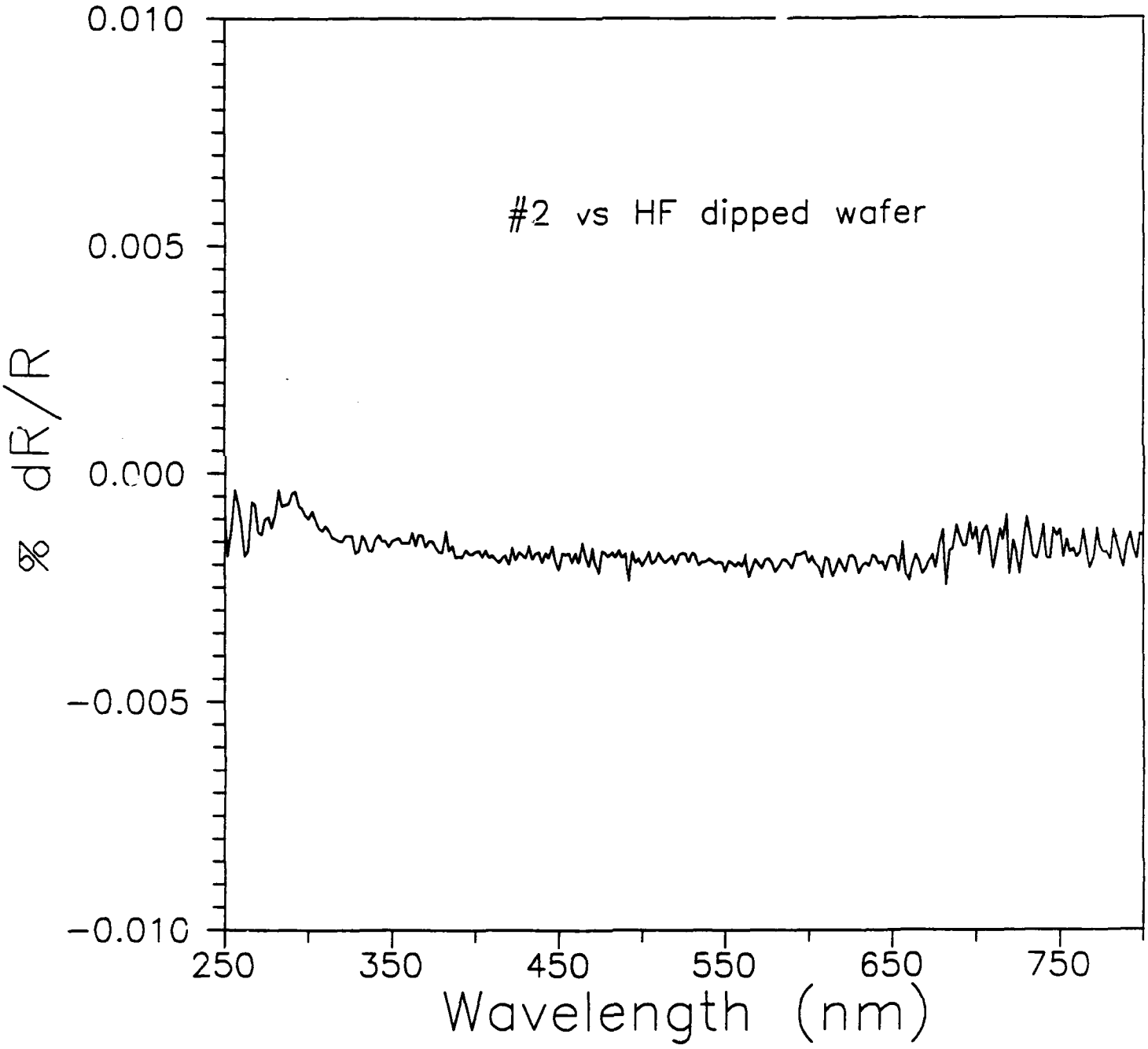
0.010
0.005
0.000
−0.005
−0.010
% dR/R
#2 vs HF dipped wafer
250
350
450
550
650
750
Wavelength (nm)

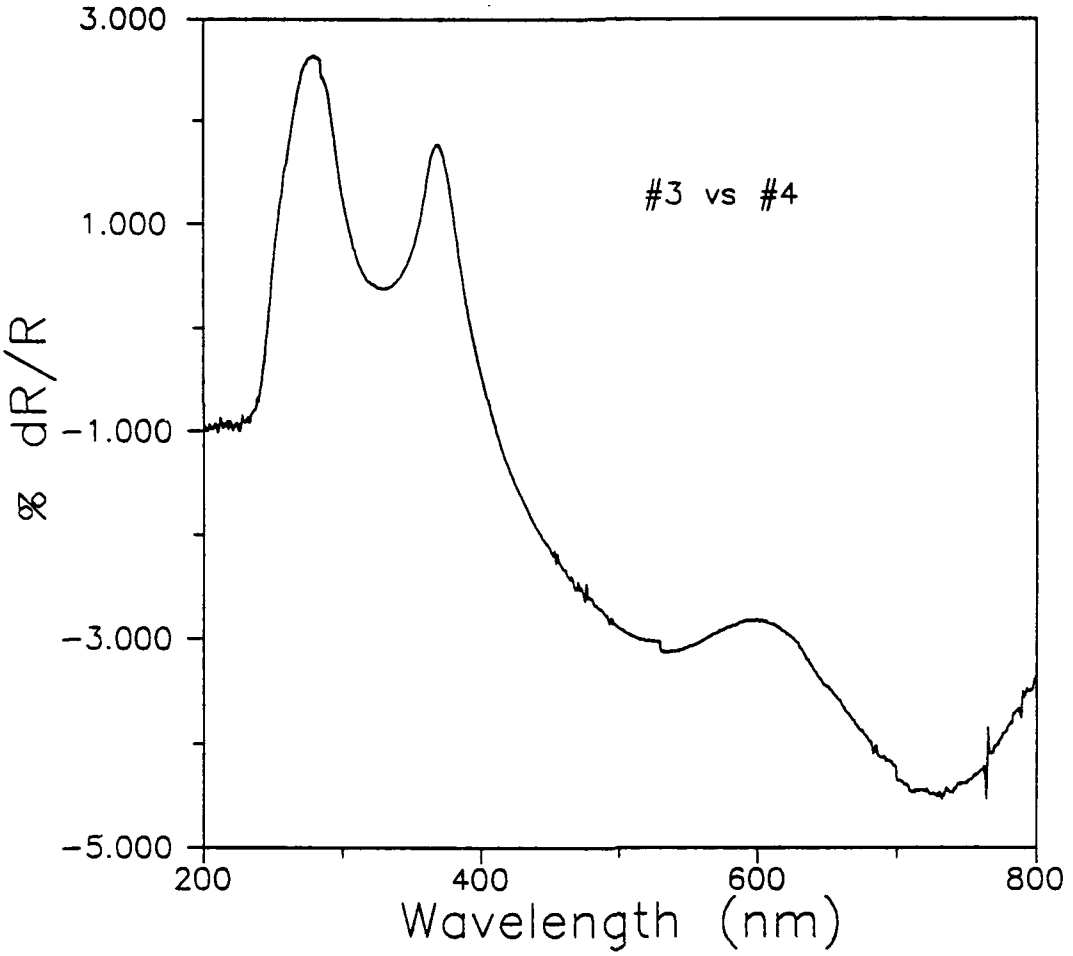
3.000
1.000
-1.000
-3.000
-5.000
% dR/R
#3 vs #4
200
400
600
800
Wavelength (nm)

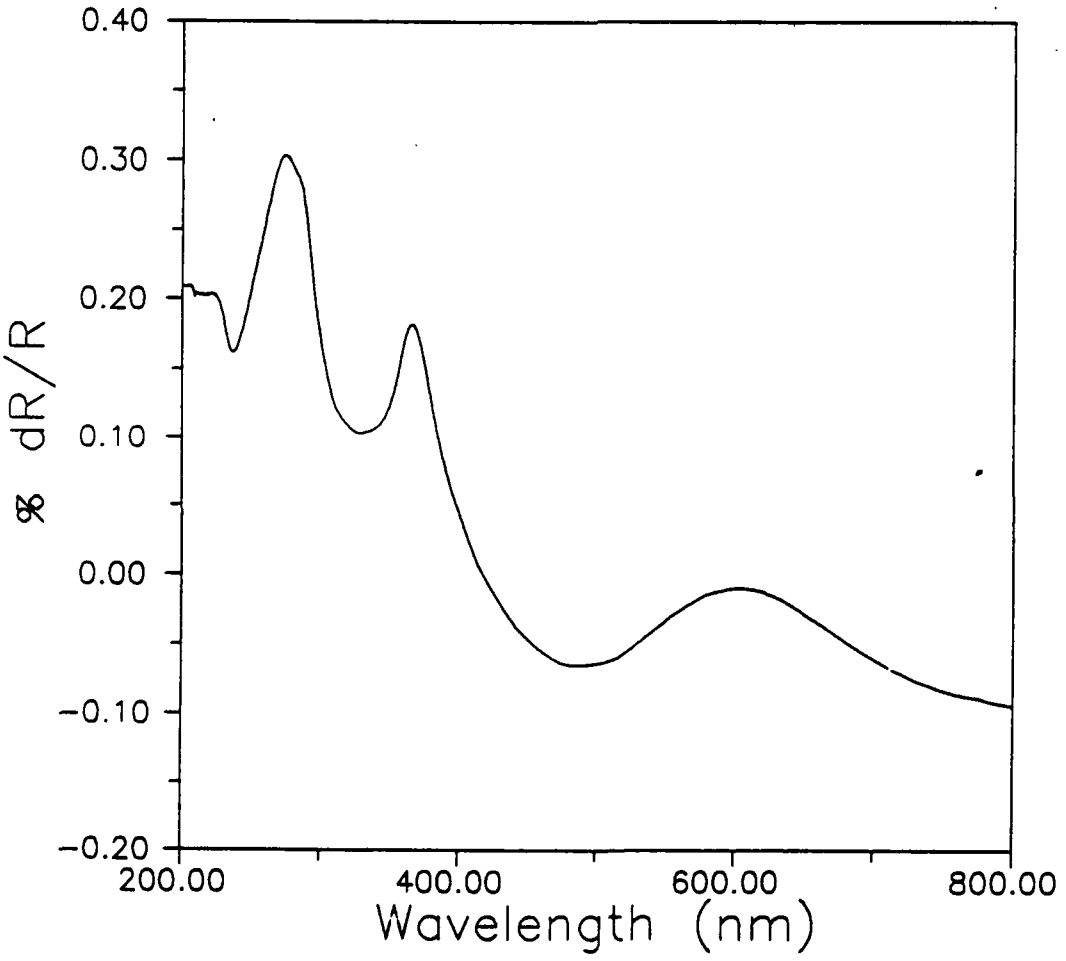
0.40
0.30
0.20
0.10
0.00
-0.10
-0.20
% dR/R
200.00
400.00
600.00
800.00
Wavelength (nm)

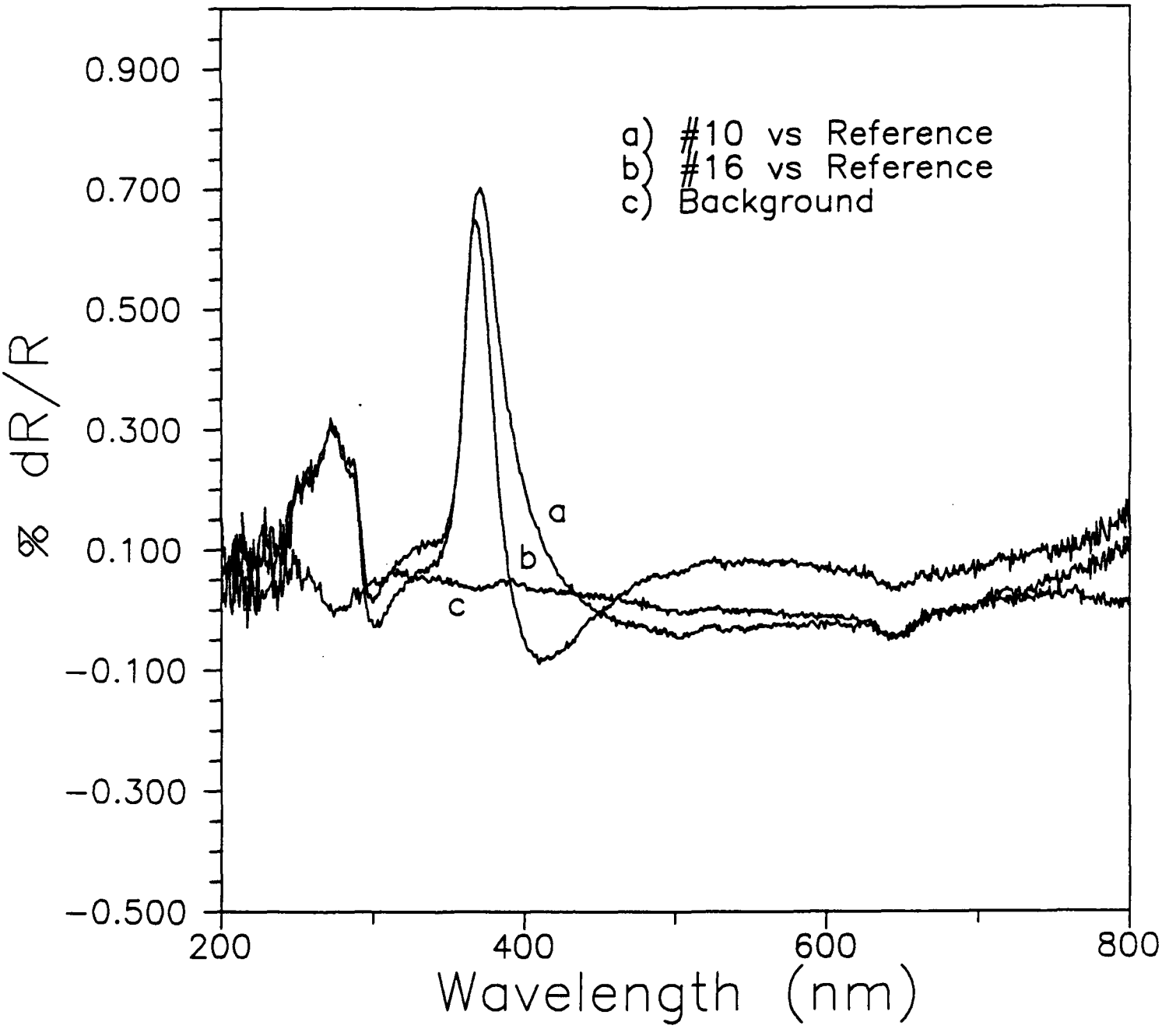
0.900
0.700
0.500
0.300
0.100
−0.100
−0.300
−0.500
% dR/R
200
400
600
800
Wavelength (nm)
a) #10 vs Reference
b) #16 vs Reference
c) Background
a
b
c

Difference from Unannealed Samples

Preamorphized and Non-preamorphized

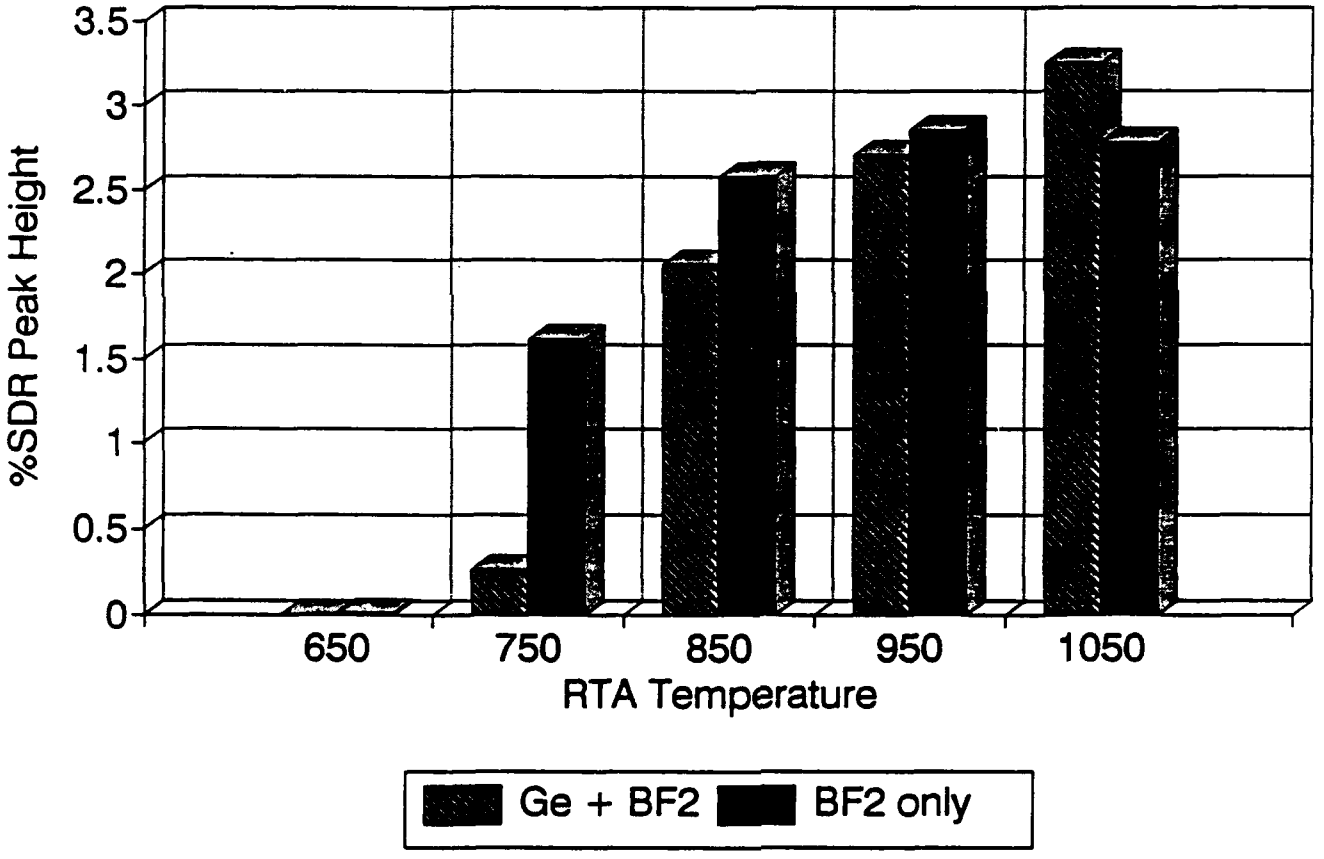

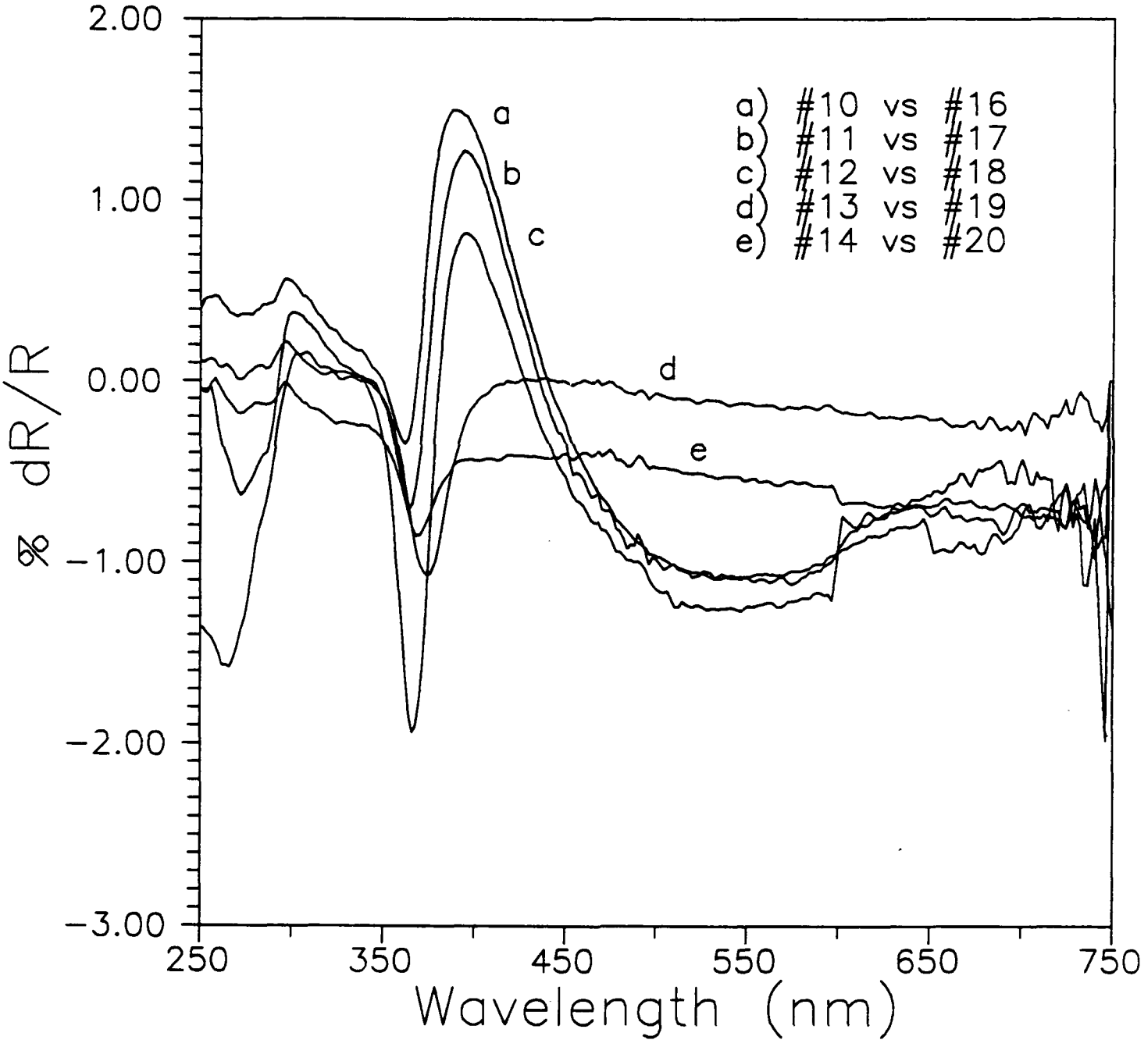
2.00
1.00
0.00
−1.00
−2.00
−3.00
% dR/R
250
350
450
550
650
750
Wavelength (nm)
a
b
c
d
e
a) #10 vs #16
b) #11 vs #17
c) #12 vs #18
d) #13 vs #19
e) #14 vs #20

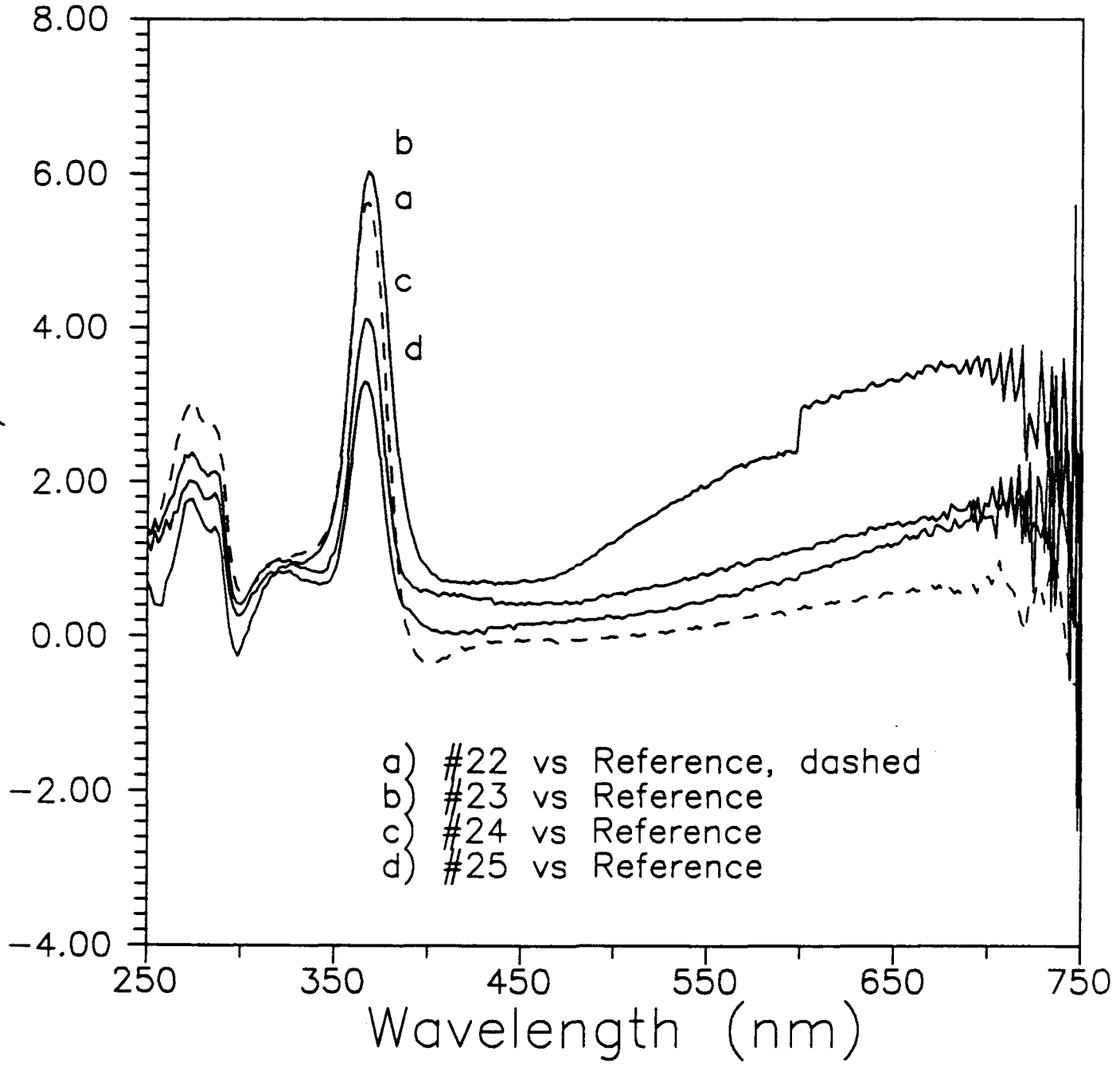
8.00
6.00
4.00
2.00
0.00
−2.00
−4.00
% dR/R
250
350
450
550
650
750
Wavelength (nm)
b
a
c
d
a) #22 vs Reference, dashed
b) #23 vs Reference
c) #24 vs Reference
d) #25 vs Reference

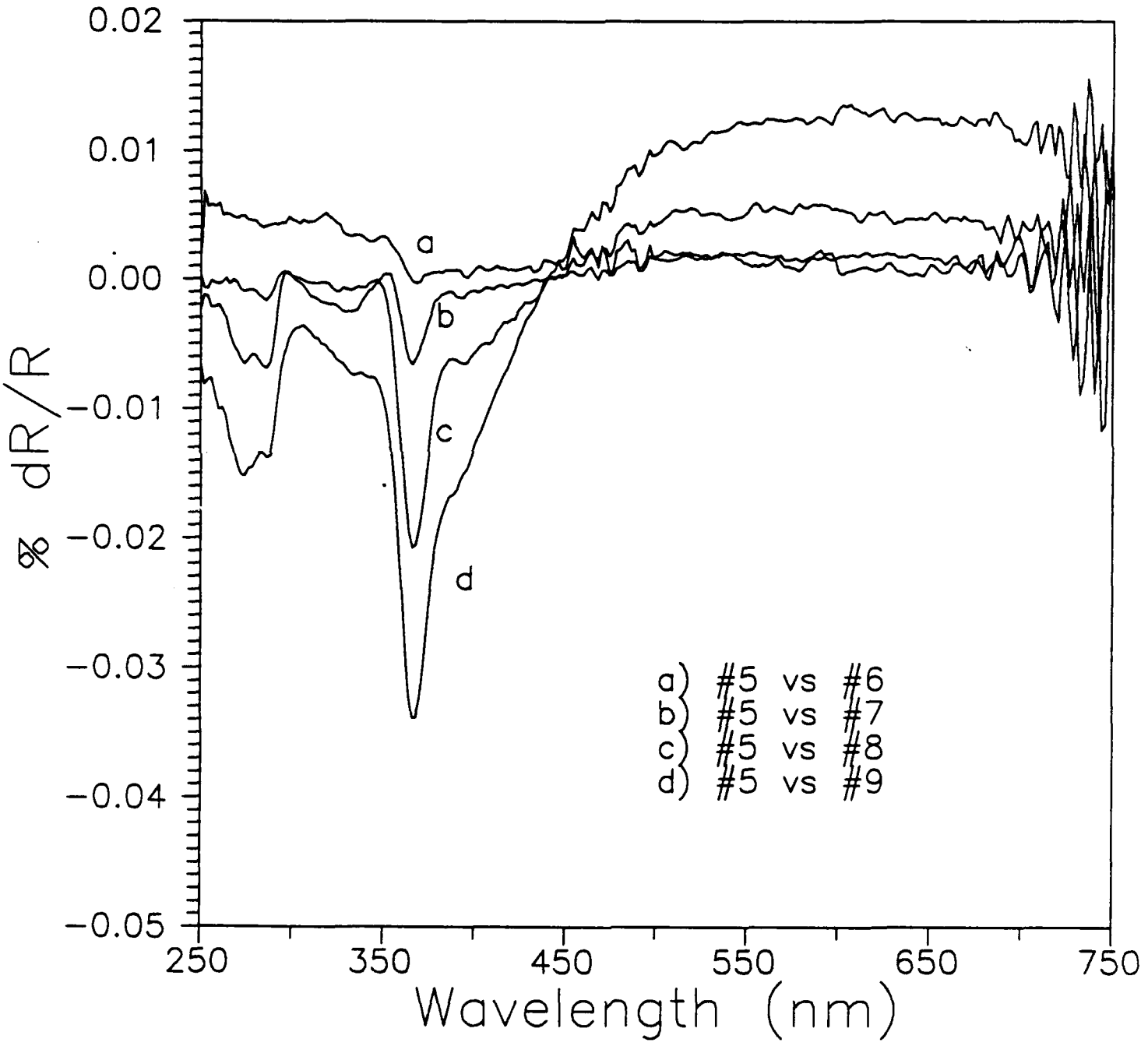
0.02
0.01
0.00
−0.01
−0.02
−0.03
−0.04
−0.05
% dR/R
250
350
450
550
650
750
Wavelength (nm)
a
b
c
d
a) #5 vs #6
b) #5 vs #7
c) #5 vs #8
d) #5 vs #9

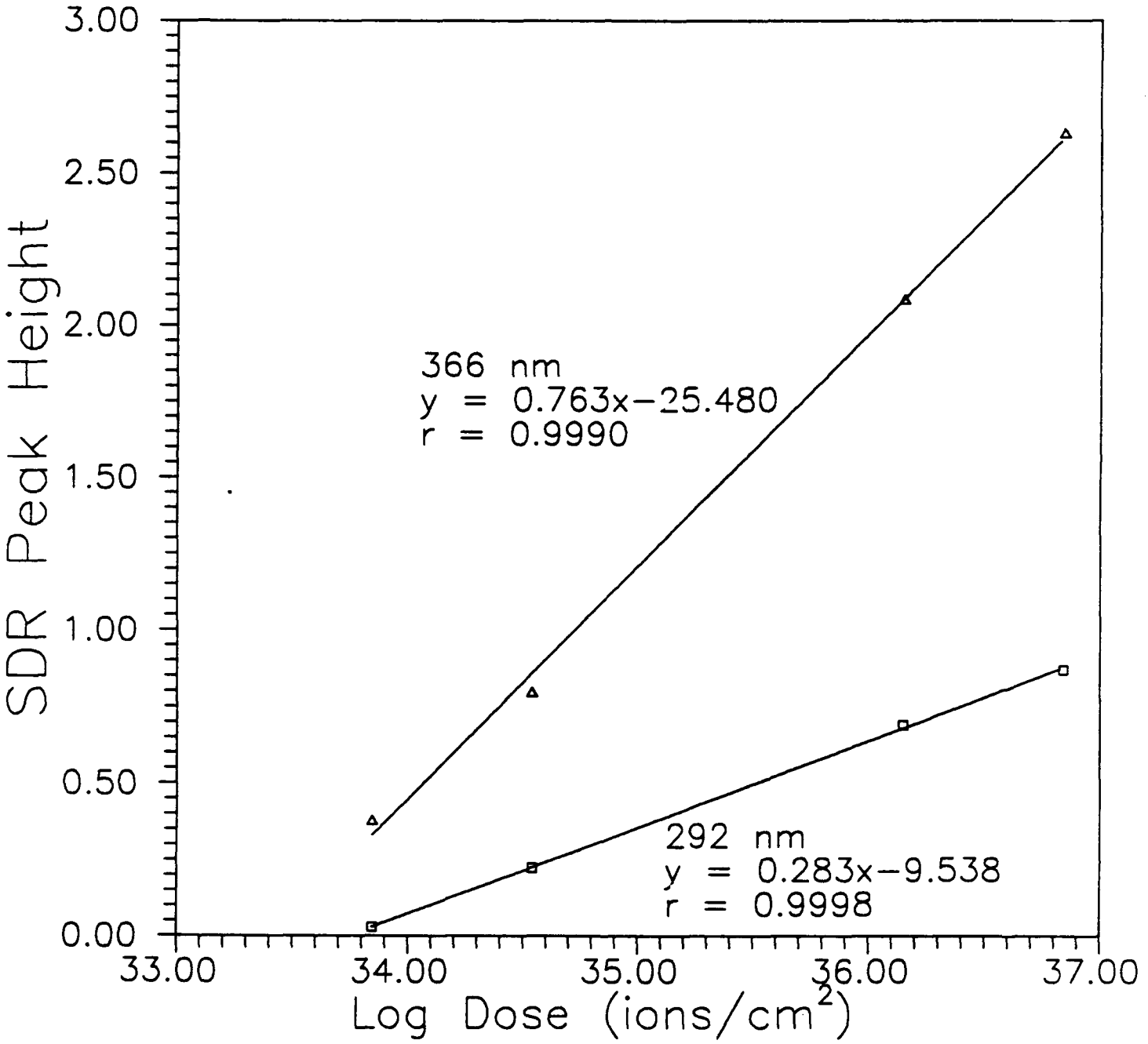
3.00
2.50
2.00
1.50
1.00
0.50
0.00
SDR Peak Height
366 nm
y = 0.763x−25.480
r = 0.9990
292 nm
y = 0.283x−9.538
r = 0.9998
33.00
34.00
35.00
36.00
37.00
Log Dose (ions/cm²)

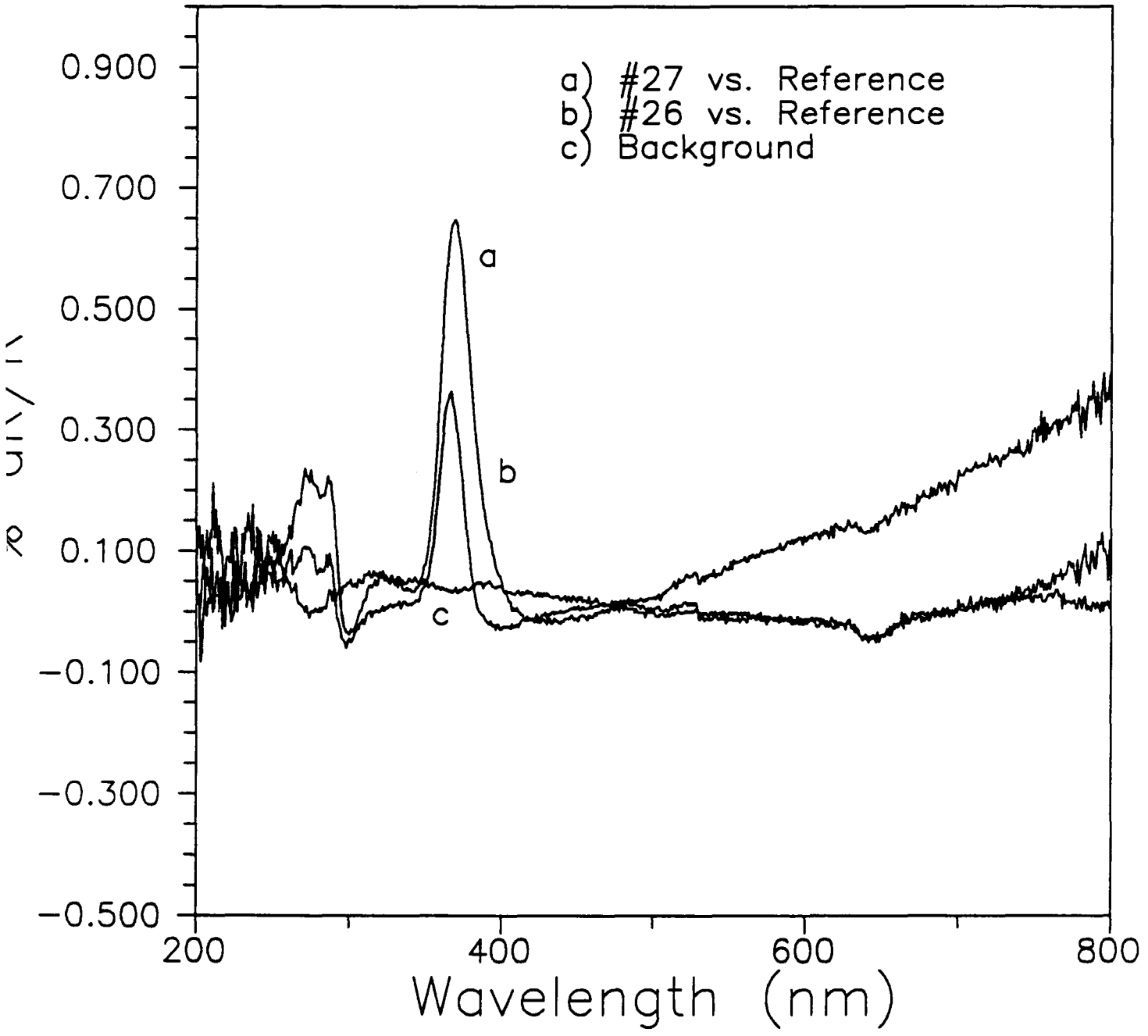
a) #27 vs. Reference
b) #26 vs. Reference
c) Background
a
b
c
0.900
0.700
0.500
0.300
0.100
−0.100
−0.300
−0.500
200
400
600
800
Wavelength (nm)

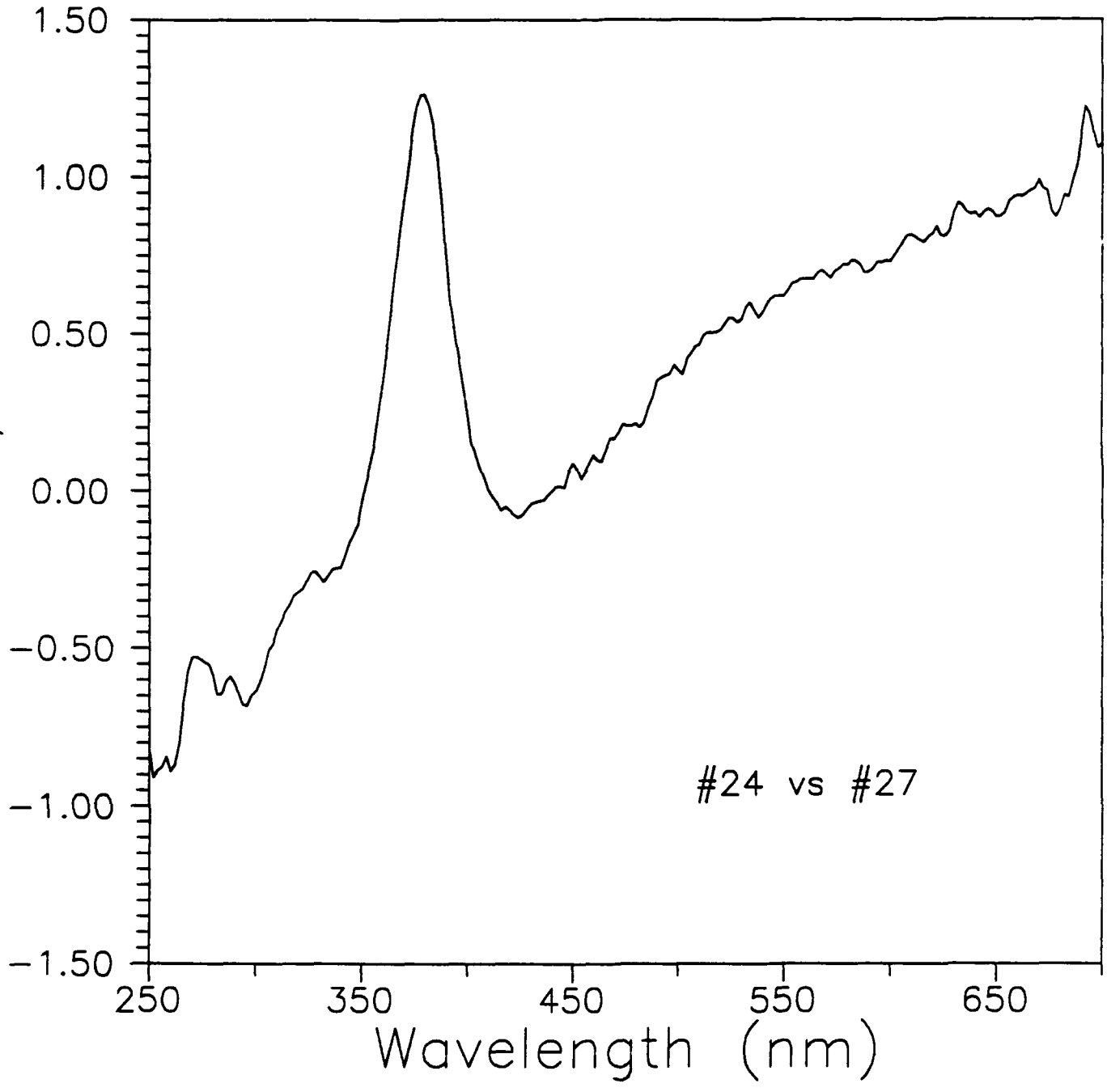
1.50
1.00
0.50
0.00
−0.50
−1.00
−1.50
250
350
450
550
650
Wavelength (nm)
#24 vs #27

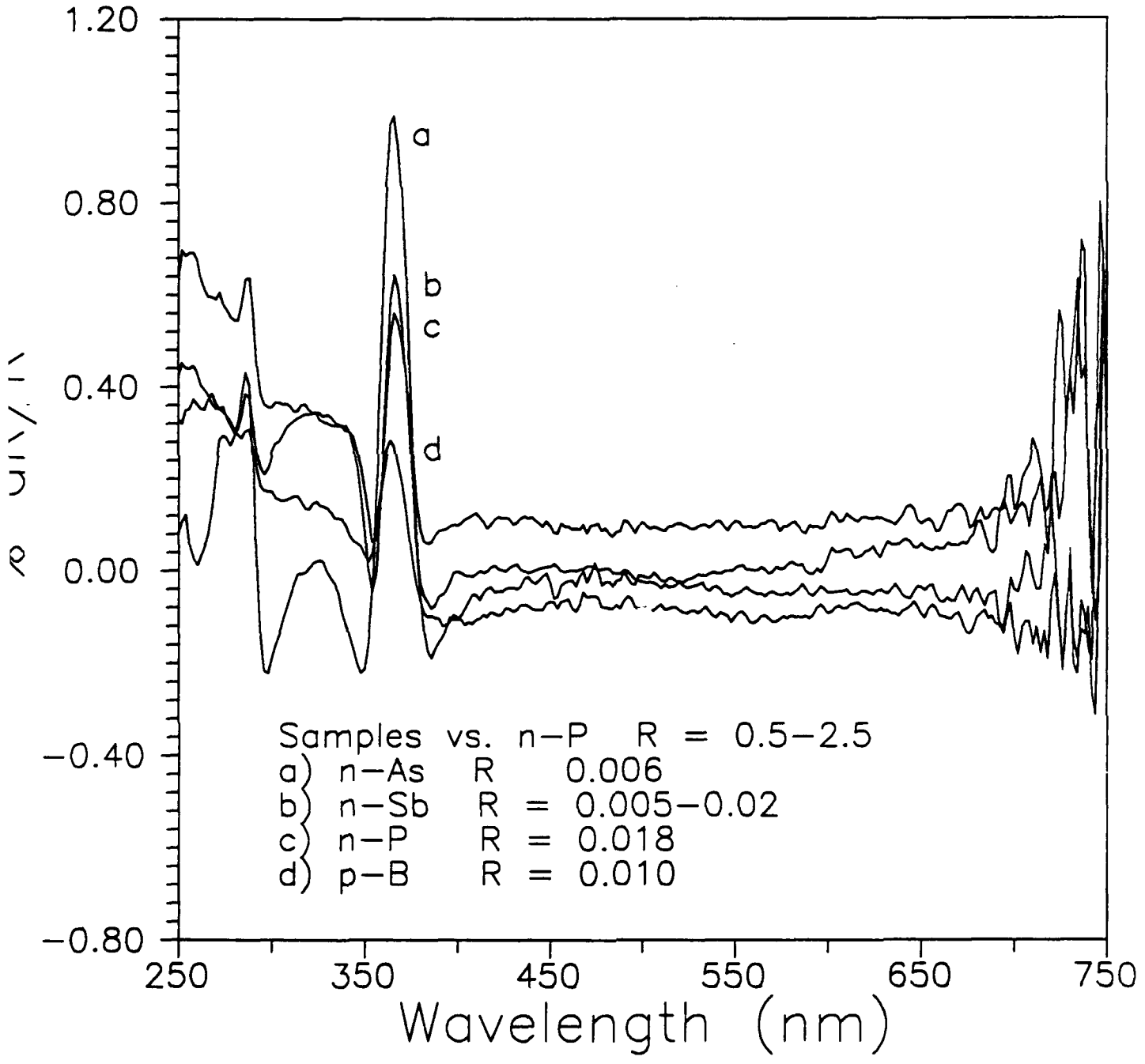
1.20
0.80
0.40
0.00
−0.40
−0.80
250
350
450
550
650
750
Wavelength (nm)
a
b
c
d
Samples vs. n−P R = 0.5−2.5
a) n−As R 0.006
b) n−Sb R = 0.005−0.02
c) n−P R = 0.018
d) p−B R = 0.010

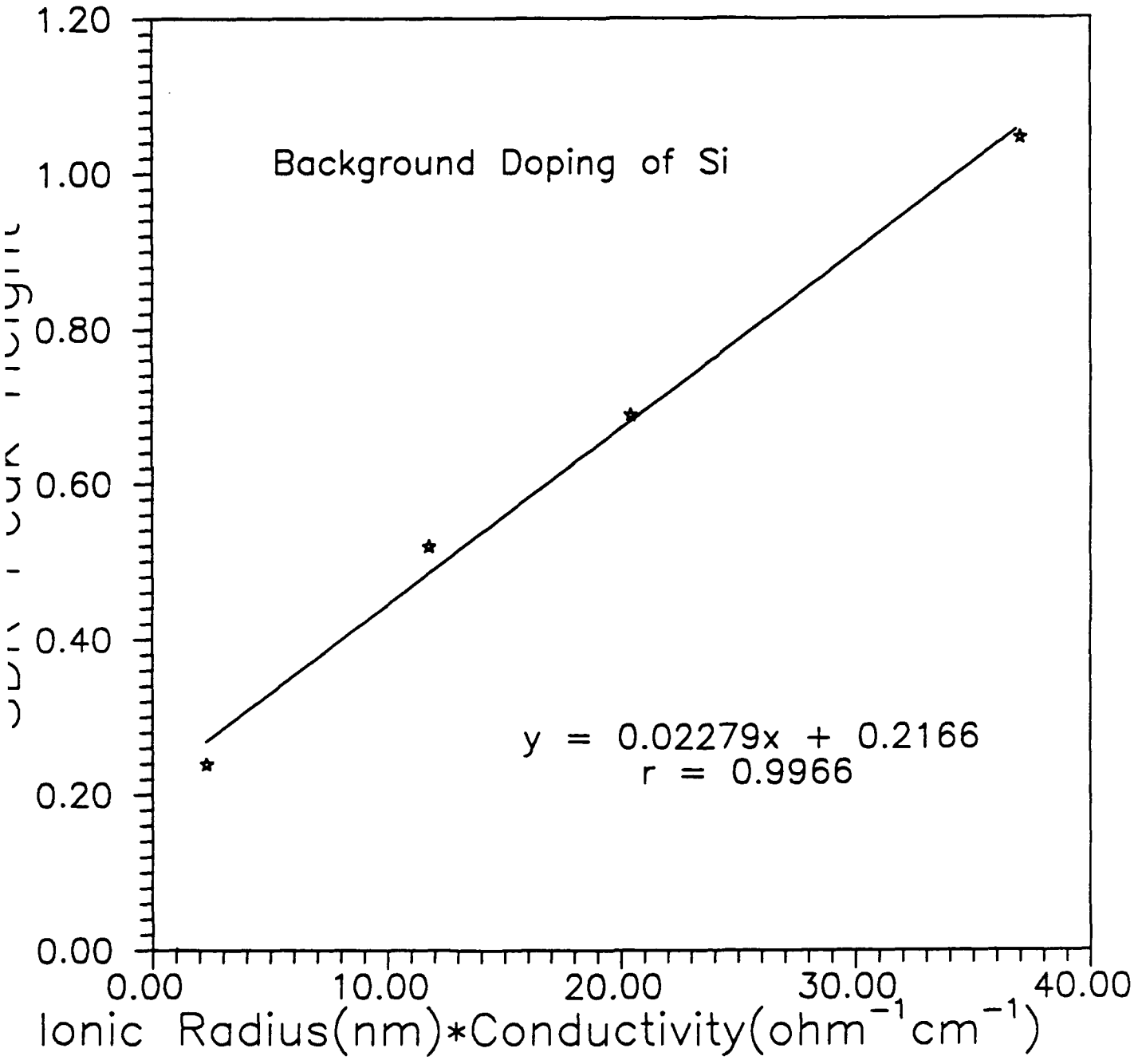
Background Doping of Si
y = 0.02279x + 0.2166
r = 0.9966
1.20
1.00
0.80
0.60
0.40
0.20
0.00
0.00
10.00
20.00
30.00
40.00
Ionic Radius(nm)*Conductivity(ohm^{-1}cm^{-1})